Infrared Study of Heat Dissipation under Fatigue Crack Propagation

O. Plekhov, M. Bannikov, A. Terekhina, A. Fedorova

Physical foundation of strength – Institute of continuous media mechanics RAS – str. Ak. Koroleva 1 – 614013 Perm (Russia), e-mail: poa@icmm.ru

ABSTRACT. *The paper is devoted to an infrared thermography study of heat dissipation in titanium alloy Ti-6Al-4V under cyclic loading. The modern infrared camera allows us to investigate the temperature evolution at fatigue crack tip with high spatial and time resolution (space resolution is 0.1 mm, time resolution is up to 500 Hz, temperature sensitivity is 0.025 ^0C). The shape and intensity of the heat dissipation zone at the fatigue crack tip are defined. It is shown that the spatial form and time evolution of the dissipation zone do not correspond to the simple theoretical models. Based on the results of comparative analysis of the experimental data and equations of the linear fracture mechanics the procedure of stress intensity factor calculation has been proposed.*

INTRODUCTION

Heat dissipation caused by the evolution of structural defects in material under cyclic deformation is the subject of intensive research over the period of the last few decades. At present, it is well known that in materials under cyclic deformation, fatigue cracks are initiated in the area of plastic deformation localization and lead to an intensive heat dissipation. With the advent of infrared thermography [1], detection of the crack initiation process becomes possible at an early stage.

The method of infrared thermography can be considered as an universal experimental tool for studying thermodynamics of the defect evolution in metals under plastic deformation and failure [2-5]. The application of this technique allows one to detect the time of the fatigue crack initiation and obtain detailed information about the process of its propagation of [6,7].

Nevertheless, some of the well-known effects accompanying the processes of fatigue crack initiation and propagation are not sufficiently investigated. In particular, the nonlinearity of the thermo-elasticity effect accompanied by a decrease of specimen temperature under quasi-static tension is still a frequently discussed issue. However, this effect is of great interest from the standpoint of studying the asymptotic of stress distribution at the crack tip and verification of the linear fracture mechanics models of crack propagation.

This work is devoted to the investigation of thermo elastic and thermoplastic effects at the fatigue crack tip. The absence of a detailed experimental study of the effect of thermoelasticity in metals encourages the authors to carry out a series of experiments on smooth specimens in order to verify the adequacy of the classical equations of thermoelasticity. Based on these results we proposed the algorithms to calculate the heat dissipation at the crack tip and estimate the stress intensity factor.

We experimentally detected cooling effects caused by elastic deformation of the material and investigate the stress distribution at the fatigue crack tip. High-speed infrared monitoring allows us to determine the intensity and shape of the energy dissipation zone caused by plastic deformation at the crack tip, as well as to compare the rate of energy dissipation for different stress levels.

EXPERIMENTAL CONDITIONS AND MATERIAL UNDER INVESTIGATION

The material under investigation is the commercial titanium alloy Ti-6Al-4V. The specimens were manufactured from a titanium sheet 3 mm thick. The geometry of smooth and cracked specimens are shown in Figure 1.
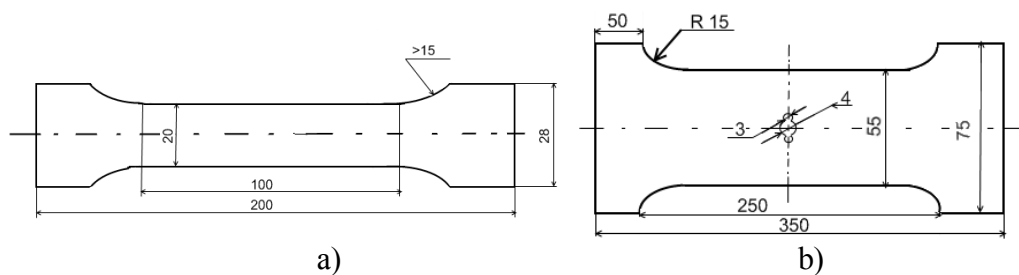

Figure 1. Specimen geometries for investigation of thermoelastic effect (a), heat dissipation under crack propagation (b).

Mechanical tests were carried out using 100 kN servo-hydraulic machine Bi-00-100. The strain was measured by an axial extensometer - Bi-06-304 with an accuracy of ± 1,5 mm.

To study thermal effects at the crack tip, the specimen was pre-weakened by holes (Fig. 1b). The fatigue crack (about 10 mm) was initiated at the initial stage of the experiment by high amplitude cyclic loading of the specimens at the average stress of 215MPa, stress amplitude of 238 MPa and loading frequency of 20 Hz. Then the load was decreased to slow down the rate of crack propagation, which allows a detailed analysis of the heat generation processes at the crack tip.

To study the process of thermoelasticity, the specimens were loaded in the elastic range at the frequencies of 1, 5 Hz and different stress amplitudes ranging from 100 to 350 MPa with the coefficient of cycle asymmetry R = 0.

The temperature evolution was recorded by the infrared camera FLIR SC 5000 at the frequencies ranging from 350 to 950 Hz and a minimum spatial resolution of $2 \cdot 10^{-4}$m. Calibration of the camera was made based on the standard calibration table.

During the experiment the grips and the specimen were shielded from the external heat sources by a special screen. The surface of the specimens was polished in several stages by the abrasive paper (at the final stage of polishing the grit size does not exceed 3 μm). Before starting the experiment, the polished surface was covered by a thin layer of amorphous carbon.

TEMPERATURE EVOLUTION ON SMOOTH SPECIMEN SURFACE UNDER ELASTIC CYCLIC LOADING

Figure 2a presents the Fourier expansion of the temperature signal from the smooth specimen surface. The second harmonic amplitude of order of 10^{-3} can be readily separated from this data.

The nonlinear thermoelastic equation [7] is used to describe the second harmonic of temperature evolution. Assuming that the elastic material constants are the function of temperature we can write

$$
\text{Log} T_t = \left(-\frac{\beta(1-2\nu)}{\rho c} + \lambda_T \frac{\sigma_0}{(3\lambda+2\mu)^2 \rho c} + 2\mu_T \frac{\sigma_0(1.5\lambda^2 + 2\lambda\mu + \mu^2)}{\mu^2(3\lambda+2\mu)^2 \rho c} \right) \Delta\sigma\omega \cos\omega t +
$$
$$
+ \left(\frac{\lambda_T}{2(3\lambda+2\mu)^2 \rho c} + \mu_T \frac{(1.5\lambda^2 + 2\lambda\mu + \mu^2)}{\mu^2(3\lambda+2\mu)^2 \rho c} \right) \Delta\sigma^2 \omega \sin 2\omega t \tag{1}
$$

where λ_T, μ_T is the first derivative of the Lame constants with respect to temperature.
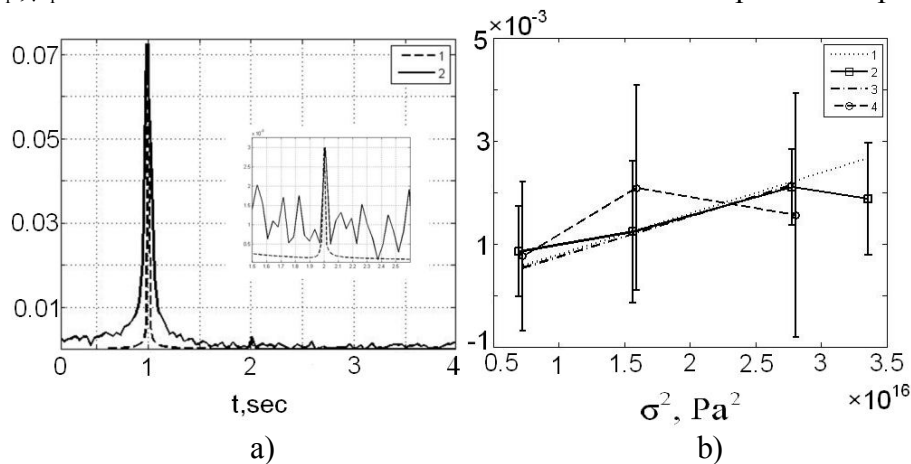

Figure 2. a) Spectra of the experimental and theoretical temperature signals (1 - solution of the equation (1), 2 - experimental data).
b) second harmonic of the temperature spectrum versus the square of the stress amplitude (for frequency of 1 Hz: 1 - solution of equation (1), 2 - experimental data; for frequency of 5 Hz, 3 - solution of equation (1), 4 - experimental data).

Figure 2b shows the results of a comparative analysis of the experimental data and the numerical solution of equation (1) for confidence intervals 0.95. From the analysis of the data presented in Figure 2 we can conclude that the second harmonic is steadily observed in the experiment. The accuracy of the experiment did not allow us to verify the theoretically predicted linear time dependence of the second harmonics.

THERMO-PLASTIC EFFECT INTO FATIGUE CRACK TIP

Figure 3 shows the points, at which qualitative changes are observed in the temperature field in the direction of crack propagation. Figure 4 presents the corresponding temperature distribution on the specimen surface.
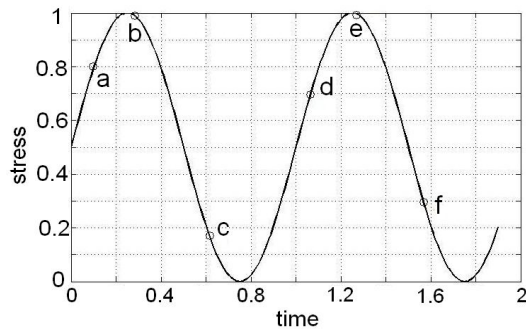

Figure 3. Stress versus time plot for temperature distributions presented in Figure 4.
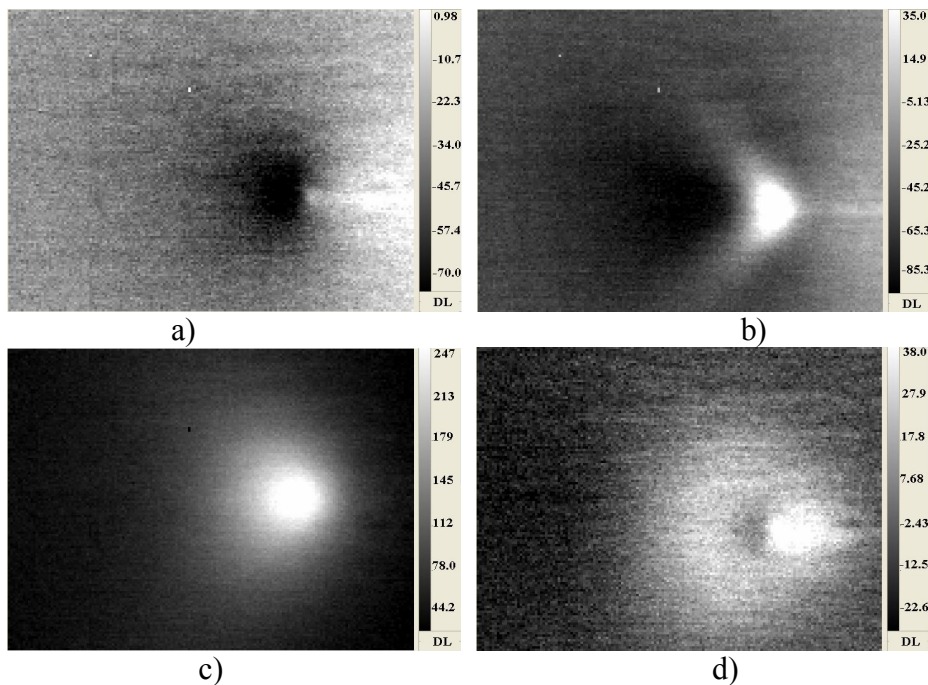

Figure 4. Temperature distributions on the specimen surface at the crack tip at different times (Figure 3).

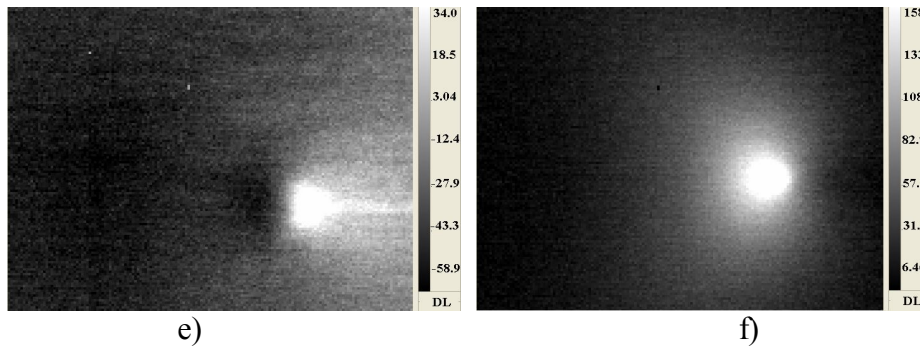e)   f)

Figure 4 (second part). Temperature distributions on the specimen surface at the crack tip at different times (Figure 3). The temperature plotted in DL (digital levels, 100 DL corresponds to one Celsius degree)

An increase in the stress at the crack tip forms a thermoelastic zone of low temperature (Fig. 4a). Then, one can observe the formation of an active heat zone caused by plastic deformation (Fig. 4b). The subsequent evolution of the heat dissipation zone is presented in figures 4c-4f. At the beginning of the second cycle of deformation a low-temperature zone appears in the center of the heat dissipation zone due to a thermoelastic effect (Fig. 4d). It is important to note that the shape of the plastic deformation zone during the second cycle (cyclic plastic deformation zone) is different from the plastic deformation zone observed during the first cycle (quasistatic plastic deformation zone) (Figure . 4b, f).

Figure 5 shows the evolution of the maximum temperature, specific heat power and stress at the crack tip in the process of loading (220 MPa stress amplitude, mean stress of 212 MPa and a frequency of 10 Hz). The indications of the displacement sensor mounted at different crack edges clearly demonstrate that the crack opening varies in phase with the applied stress.
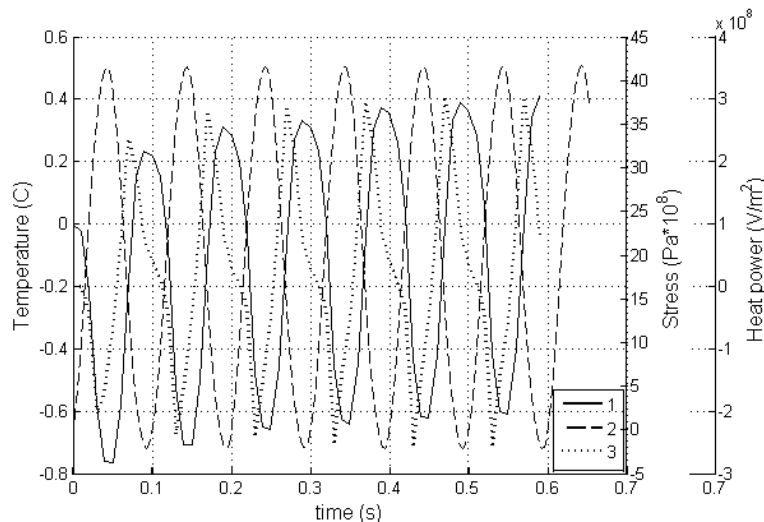

Figure 5. Evolution of maximum temperature at the fatigue crack tip (1), stress (2), and specific heat power (3) under cyclic deformation.

The analysis of the data presented in Fig.5 shows that the maximum applied stress and the maximum intensity of heat dissipation at the tip of the fatigue cracks do not coincide in time.

Logically, to compare the shape of the plastic deformation zone with the predictions of the linear fracture mechanics, we should analyze the shape of the plastic deformation zone formed during the first cycle of deformation. Infrared thermography can accurately visualize the zone of intense energy dissipation at the crack tip during the first cycle of deformation (Fig. 6).

A comparison of the observed shape of the intensive heat dissipation zone and the shape of the plastic deformation zone at the crack tip predicted by the classical solutions demonstrates that there is only a qualitative agreement between the observed zone of intensive heat dissipation at the crack tip and the predictions of the von Mises and Tresca-Saint Venant models.

Inconsistencies caused by the application of simple elastic-plastic equations to studying the temperature evolution at the crack tip restrict the range of theoretical models, which can be used for calculation of the stress intensity factor (SIF).
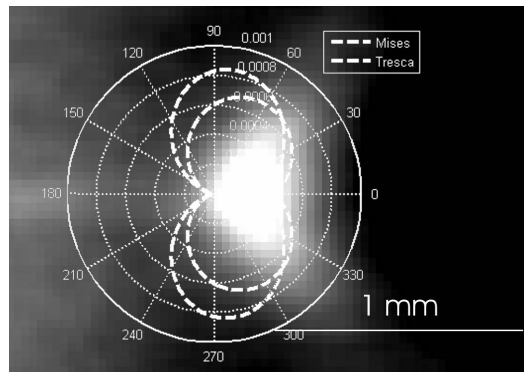

Figure 6. Heat dissipation zone at the crack tip during the first cycle of deformation and plastic deformation zone calculated based on the von Mises and Tresca-Saint Venant criteria.

To calculate the value of SIF we analyzed the low-temperature (thermoelastic) zone at the crack tip. The theoretical value of SIF can be calculated as follows:

$$K = \sigma \sqrt{\pi a} F(\alpha), \qquad (2)$$

where σ is the applied stress, a is half of the crack length, $\alpha = 2a/W$, W is the specimen width, $F(\alpha) = (1 - 0.025\alpha^2 + 0.06\alpha^4)\sqrt{\sec(\alpha\pi/2)}$.

To determine experimentally the value of SIF we can use the well know relation of thermoelasticity

$$\Delta\sigma = -\frac{\rho c}{\beta T_0}\Delta T, \qquad (3)$$

where ρ is the material density, β is the thermal expansion coefficient, c is heat capacity, ΔT is experimentally determined temperature increment near the fatigue crack tip.
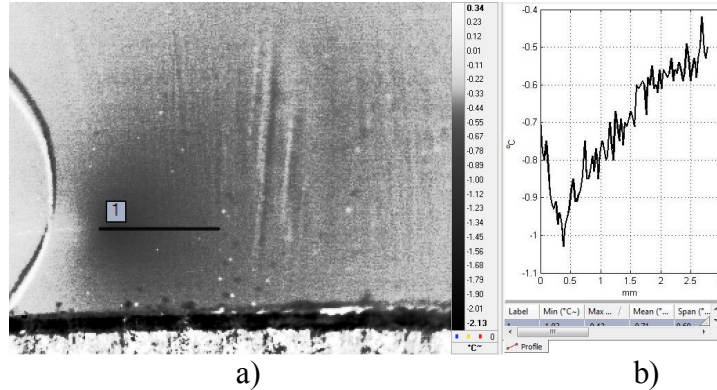

Figure 7. Temperature distribution over the specimen surface at the fatigue crack tip (a), temperature increment in the direction of crack propagation (b).
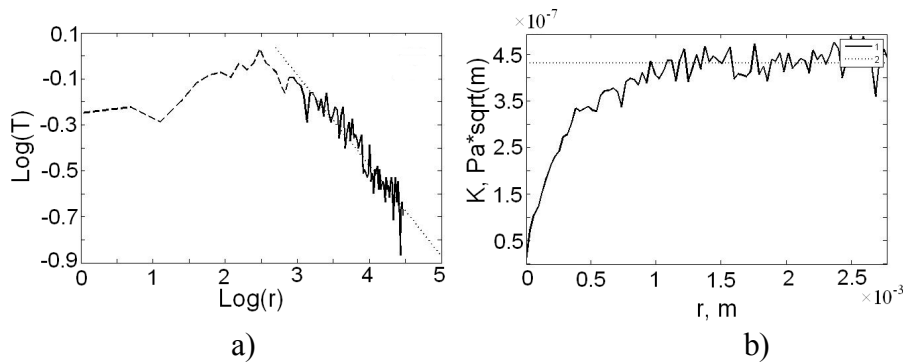

Figure 8. Temperature increment in the direction of crack propagation in log-log coordinates (a), variation of SIF with the distance from visually determined crack tip (b, horizontal line is the theoretical value of SIF).

Let us to consider the one-dimensional function $\Delta T(r)$ determined in the direction of crack propagation (Fig 7). First, it is necessary to determine the location of the crack tip. The crack has different emissivity and can be visualized by infrared thermography. However, the existence of the cohesive force zone near the crack tip complicates the problem. This zone cannot be easily observed. Let us assume that the maximum stress corresponds to the real crack tip position. In this case, we can associate the minimum temperature increment with the real position of the crack tip.

Based on equation (3) we can calculate the stress increments in the direction of crack propagation $\Delta\sigma(r) = -\dfrac{\rho c}{\beta T_0}\Delta T(r)$, which can be related with SIF

$$\Delta K = \Delta\sigma(r)\sqrt{\frac{\pi r}{2}} = -\frac{\rho c}{\beta T_0}\Delta T(r). \tag{4}$$

An example of applying equation (4) to infrared monitoring data is presented in figure 8. A slope of the last part of the plot is close to a theoretically determined value 0.5. The first part of the plot can be considered as the result of the appearance of the cohesive force zone at the crack tip. The last part of the plot gives the constant value of SIF, which coincides with value determined from equation (2).

CONCLUSIONS

Temperature evolution near the fatigue crack tip and on the smooth specimen surface has been investigated using infrared thermography. Investigation of the temperature evolution of titanium alloy Ti-6Al-4V specimens under cyclic deformation showed that the thermoelastic process is nonlinear and the generation of higher temperature harmonics can be observed experimentally. The analysis of the thermoelastic effect at the crack tip under low stress amplitude allows us to suggest an effective method for evaluating the stress intensity factor and geometry of cohesive zone at the crack tip.

The study of the thermoplastic effect at the fatigue crack tip has shown that the process of heat dissipation is essentially nonlinear. At this stage of research the results of experimental study strongly suggest that the shape of the zone of plastic deformation does not coincide with the predictions of the linear fracture mechanics, and the maximum heat is reached on the descending branch of the load.

ACKNOWLEDGMENTS.

REFERENCES

1.　　Plekhov O., Palin-Luc T., Naimark O., Uvarov S., Saintier N. (2005) *Fatigue and fracture of engineering materials and structures,* **28**, 169-178.

2.　　Rosakis P., Rosakis A.J., Ravichandran G., Hodowany J. (2000) *J. Mech. and Phys. Solids*, **48**, 581-607.

3.　　Oliferuk W., Maj M., Raniecki B. (2004) *Materials Science and Engineering A,* **374**, 77-81.

4.　　Poncelet M., Doudard C., Calloh S., Weber B., Hild F. (2010) *J. Mech. and Phys. Solids*, **58**, 578-593.

5.　　Fragione G., Geraci A., La Rosa G., Risitano A. (2002) *Int. J. Fatigue,* **24**, 11-19.

6.　　Ogasawara N., Shiratori M. (1997) *SPIE proceeding series,* **3056,** 201-213.

7.　　Jones R., Krishnapillai M., Cairns K. Matthews N. (2010) *Fatigue and Fracture of Engineering Materials and Structure,* **33**, 871-884.